Journal of Catalysis **200,** 209–221 (2001)
doi:10.1006/jcat.2001.3180, available online at http://www.idealibrary.com on IDEAL®

Determination of Adsorption and Kinetic Parameters for Methyl *tert*-Butyl Ether Synthesis from *tert*-Butyl Alcohol and Methanol

Zhang Ziyang, K. Hidajat, and Ajay K. Ray[1]

Department of Chemical and Environmental Engineering, The National University of Singapore, 10 Kent Ridge Crescent, Singapore 119260

Received July 18, 2000; revised January 22, 2001; accepted January 23, 2001; published online April 24, 2001

Methyl *tert*-butyl ether (MTBE), a high-octane blending agent for motor gasoline, is produced by reacting directly *tert*-butyl alcohol (TBA) with methanol using Amberlyst 15 ion-exchange resin, which acts as both catalyst and adsorbent. Experiments were carried out in a fixed-bed reactor in the temperature range 318–328 K using rectangular pulse input and measuring the elution profiles of TBA, MTBE, and H_2O. A mathematical model based on a quasi-homogeneous kinetics was developed, which assumes the reaction in the polymer phase to be homogeneous. The kinetic parameters, as well as the adsorption equilibrium constants of water, TBA, and MTBE in methanol together with their dependence on temperature, were determined by tuning the simulation results to fit the experimental data using a state-of-the-art optimization technique,the genetic algorithm. The model was further validated using the tuned adsorption and rate parameters to predict other experimental results. The kinetics reported in the present study were obtained under conditions free of both external and internal mass transfer resistance. The enthalpy and entropy of adsorption obtained from Arrhenius plots were found to be consistent with thermodynamics.

Key Words: **MTBE; kinetic parameters; adsorption parameters; direct synthesis; TBA; methanol.**

INTRODUCTION

Pollution from motor vehicles is responsible in industrialized nations for ozone-forming smog, hazardous carbon monoxide pollution, and other toxic air pollutants. Methyl *tert*-butyl ether (MTBE) is widely used as an oxygenate for gasoline (1) not only to enhance the octane number but also to make motor vehicle fuel burn more cleanly (replacing toxic additives like lead), thereby significantly reducing toxic tailpipe pollution (2).

MTBE was first manufactured commercially in the early 1970s in Europe by Chemische Werke Huls in West Germany and by ANIC in Italy. After the Environmental Protection Agency granted approval for MTBE blending (although recently the U.S. EPA is in favor of reduction of MTBE content in U.S. gasoline) to unleaded gasoline in the U.S.A. in 1979, rapid growth took place almost immediately since MTBE could be manufactured and blended at the refinery complex. The production and import of MTBE in the U.S.A. reached the highest levels in 1998 (3) although presently there is a ban on the use of MTBE in California. MTBE has highly favorable performance qualities from the refiner's perspective, including high octane number, low sulfur content, acceptable blending vapor pressure, high miscibility in gasoline, moderate boiling point, and stability in storage. Additionally, MTBE's cost, compared to those of other high-octane components, made it the economical choice in the refinery marketplace. Commercially, MTBE is synthesized today by reversible etherification reaction of isobutene (IB, a feedstock derived from natural gas or as a by-product of petroleum refining) with methanol at an operating temperature between 313 and 353 K under a pressure high enough to maintain the reaction system in liquid phase. Sulfonated acidic ion-exchange resin (such as Lewatit SPC 118, Amberlyst 15 or Purolite CT-115) is typically used as catalyst. The reversible reaction is represented by

$$(CH_3)_2CCH_2 + CH_3OH \rightleftharpoons (CH_3)_3COCH_3 \qquad \Delta H = -37.3\ \text{kJ/mol}. \qquad [1]$$

Numerous publications (4–15) report thermodynamics, kinetics, and reaction mechanism studies of this reaction using ion-exchange resins as catalyst under different experimental conditions. Several attempts have also been made to synthesize MTBE using a variety of zeolite catalysts such as ZSM-5 (16–19) and ZCIC-10 (20). However, a problem concerning MTBE production from isobutene is that the source of isobutene (IB) is limited to catalytic cracking and steam cracking fractions of petroleum refining. Another possible source of isobutene is isobutane dehydrogenation. Approximately 30% of MTBE production worldwide at present is made from this feedstock.

Commercially, MTBE is also produced from *tert*-butyl alcohol (TBA), a by-product of propylene oxide synthesis. There are two ways to produce MTBE from TBA,

[1] To whom correspondence should be addressed. Fax: +65 779 1936. E-mail: cheakr@nus.edu.sg.

0021-9517/01 $35.00

an indirect and a direct method. In the indirect method (ARCO process), TBA is dehydrated to IB in the first reactor according to Eq. [2],

$$(CH_3)_3COH \rightleftharpoons (CH_3)_2CCH_2 + H_2O, \qquad [2]$$

followed by reaction of IB with methanol to produce MTBE in the second reactor (10) according to Eq. [1]. In the direct method, MTBE can be produced by reacting TBA directly with methanol in one reactor in the presence of an acid catalyst in which water is also formed as a by-product:

$$(CH_3)_3COH + CH_3OH \rightleftharpoons (CH_3)_3COCH_3 + H_2O. \qquad [3]$$

The choices of solid acid catalyst for the above reaction (Eq. [3]) are (a) a variety of heteropoly inorganic solid acid catalysts (21, 22), and (b) hydrogen ion-exchange acid resins, such as Amberlyst 15 (23). To the best of our knowledge, there are no reported works on the direct synthesis of MTBE from TBA using acid resin catalyst other than the work of Matouq and Shigeo (23). Recently, another brand of Amberlyst resin (Amberlyst 35) has been found to be suitable as catalyst for many reactions. But, in this study we have used Amberlyst 15 only.

In contrast to kinetic studies of MTBE synthesis from isobutene and methanol, on which numerous papers have been published during the last 20 years, direct reaction of TBA and methanol to produce MTBE drew little attention. In the open literature, Matouq and Shigeo's work (23) seems to be the only one reported. They studied the direct synthesis of MTBE from methanol and TBA in a stirred batch reactor at different temperatures under atmospheric pressure using Amberlyst 15 ion-exchange resin as catalyst. Their experimental results showed that catalyst sizes and rotation speed had no significant effects on reaction rates. They found that the liquid film diffusion resistance and particle internal diffusion resistance are negligible. They proposed a reaction mechanism in which three reactions take place and determined rate expressions based on simple kinetics. However, in developing the kinetics, the polymer resin catalyst was treated as a common dissolved electrolyte, and the reaction was regarded as homogeneous in the liquid phase. However, it is well-known that resin catalyst can offer a degree of adsorption selectivity that is unattainable in homogeneous acid or base catalysis. Therefore, the advantages of solid resin catalysts over the traditional liquid acid or base catalysts were ignored.

The economics of many industrial chemical processes are unfavorably influenced by the equilibrium limitations of the reactions involved, which results in low yield and/or selectivity. This can be seen in the high additional costs required for the separation of nonconverted reactants from the reactor outlet product and their recycling to the reactor inlet. This can be circumvented by the use of a simulated countercurrent moving-bed chromatographic reactor (SCMCR), a device for carrying out chemical reaction and separation simultaneously in a fixed bed (24, 25). These are novel reactors in which separation takes place at the site of chemical reaction to improve product purities and conversions beyond those prescribed by thermodynamic equilibrium. The integration of reaction and separation not only reduces the capital and operating costs, but also results in better yields and selectivity, reduces adsorbent requirement, and minimizes problems associated with product inhibition in addition to the added advantages of performing reactions at low pressure and temperature. The primary objective of our research in studying the direct synthesis of MTBA from TBA and methanol is to determine to what extent the moving-bed reactor advantages of high purity and favorable equilibrium shifts are retained in SCMCR operations. In this paper, we report an experimental investigation to determine the adsorption and kinetic parameters of this reaction.

REACTION KINETICS AND ADSORPTION ISOTHERM

Numerous publications (4–15) exist on the reaction mechanism and kinetic and thermodynamic studies of the reaction given by Eq. [1] using ion-exchange resins as catalyst. Ancillotti *et al.* (4) concluded from experimental studies on the MTBE synthesis that the reaction rate is negative order dependent on methanol concentration below 4 mol/l, while it is zero-order dependent above 4 mol/l due to a shift in the reaction mechanism. At low methanol concentration, the undissociated sulfonic acid group is active, while the solvated protons become the catalytic agents at increasing methanol concentration as the network of hydrogen-bonded SO_3H groups is broken down by the excess alcohol present in the pores of the resin owing to selective swelling. In addition, they concluded that the olefin protonation was the rate-limiting step and the rate is first-order dependent on the concentration of IB (9). However, no kinetic expression was reported.

As for the kinetic rate models for the reaction (Eq. [1]) in the presence of resin catalysts, several papers have been published recently based on either the homogeneous (8, 26) or the heterogeneous (6, 10–12, 14, 15) model, which were derived mainly from either the Langmuir–Hinshelwood (LH) or the Eley–Rideal (ER) mechanism. The rate equations were described as a function of either concentrations or activities. It can be generalized from the previous works that the reaction proceeds quasi-homogeneously when methanol is present in a large excess, and the rate-limiting step is the protonation of isobutene. The resin is completely swollen by the polar protophilic species methanol, and the polymer-fixed acid is dissociated completely. However, when methanol concentration is decreased, the catalytic agent is the sulfonic acid group itself and a quasi-heterogeneous phenomenon begins to conquest. In most heterogeneous kinetic models, the rate-limiting step is the

surface reaction either between methanol and isobutene both adsorbed on the resin (LH mechanism), or between the methanol adsorbed on the resin and the isobutene present in the solution. In a recent article, Tejero *et al.* (15) suggested that a transition from the ER to the faster LH mechanism takes place, depending on the methanol concentration in the liquid phase.

Mazzotti *et al.* (27) reported an interesting kinetic study for a similar reaction system, esterification of ethanol and acetic acid with ethyl acetate and water as products using Amberlyst 15 ion-exchange resin as catalyst. They (27) put forward a quasi-homogeneous model based on the composition in the polymer phase. The polymer phase concentrations were related to those in the liquid phase by equating the activities of each component in the two phases. The activities were estimated using UNIFAC for the liquid phase, and the extended Flory–Huggins model for the polymer phase. The parameters were fitted to adsorption equilibrium experimental results of four binary systems where no reactions were involved. Coupled with their kinetic model, their phase equilibrium model was successful in predicting the breakthrough curves of individual components in a fixed-bed chromatographic reactor (28). However, their phase equilibrium model is impractical for most adsorption systems, as nonreactive binary mixtures are scarce, besides its complexity and inconvenience in computation. Hence, the method is not suitable for predicting the phase equilibrium of the reacting system and is not used in the present study.

In order to develop an overall kinetic expression for the reaction system studied in this work, analysis of the three reactions proposed by Matouq and Shiego (23) is indispensable. For the TBA–methanol–acid ion-exchange system, the following three reactions may take place:

$$\mathrm{TBA} \rightleftharpoons \mathrm{IB} + \mathrm{H_2O} \quad [4]$$

$$\mathrm{IB} + \mathrm{MeOH} \rightleftharpoons \mathrm{MTBE} \quad [5]$$

$$\mathrm{TBA} + \mathrm{MeOH} \rightleftharpoons \mathrm{MTBE} + \mathrm{H_2O}. \quad [6]$$

If IB produced in the first reaction (Eq. [4]) is consumed instantaneously and completely according to the second reaction (Eq. [5]), then the overall reaction can be described by Eq. [6]. However, in our experimental studies, gas bubbles (isobutene) were detected in the effluent from the packed-bed reactor as well as when experiments conducted in a well-stirred batch reactor using the same catalyst. Hence, the intermediate product, isobutene, is not consumed completely, possibly because the rate of formation of IB in the first reaction (Eq. [4]) is faster than that of the consumption by the second reaction (Eq. [5]). In this case, the third reaction (Eq. [6]) takes place in addition to reactions 1 and 2 (Eqs. [4] and [5]).However, it can be noticed from the above three reaction expressions that the overall TBA consumed equals the overall rate of H_2O produced, and similarly for methanol consumed and MTBE produced. Based on the above, the overall reaction can be described by the following equation,

$$n(\mathrm{CH_3})_3\mathrm{COH} + \mathrm{CH_3OH} \rightleftharpoons (\mathrm{CH_3})_3\mathrm{COCH_3} + n\mathrm{H_2O} + (n-1)(\mathrm{CH_3})_2\mathrm{CCH_2}, \quad [7]$$

where n (usually greater than 1) is an unknown parameter, which indicates the ratio of reaction rates between the first (Eq. [4]) and the second (Eq. [5]) reactions and the amount of isobutene produced. However, if isobutene produced is neglected, n is equal to 1, and Eq. [7] reduces to Eq. [6]. It should also be noted that although methanol is one of the reactants, it also acts as carrier solvent and is usually present in excess. Its concentration varies very little in the entire reaction process and, therefore, can be regarded as constant. The concentration of isobutene in the solid phase can also be neglected for its low boiling point, being present in a trace amount, and most importantly, it has very low affinity toward the ion-exchange resin. To the best of our knowledge, there is no reported work in the literature on the kinetics of this reaction. Determination of adsorption and kinetic parameters of Eq. [7] is the main objective of this work.

Ancillotti *et al.* (4, 5) proposed a reaction mechanism for the reaction (depending on the concentration of methanol and its proportion to other reactants) between methanol and IB (Eq. [1]) to produce MTBE catalyzed by the same ion-exchange resin (Amberlyst 15). They concluded that the reaction is catalyzed mainly by solvated proton when methanol is present in large excess compared to IB. The network of hydrogen-bonded SO_3H groups can be broken by methanol, which is usually present at high concentration in the pore liquid. The dissociated proton is distributed evenly in the pore liquid. Likewise, the reaction given by Eq. [7] can also be visualized as a quasi-homogeneous reaction, or homogeneous in the polymer phase. The adsorbed TBA reacts with methanol to produce MTBE, H_2O, and IB catalyzed by the dissociated proton present in the pore of the ion-exchange resin particle, which is initially saturated with methanol. The concentrations of MTBE and H_2O in the polymer phase depend on their adsorption equilibrium, while the nonadsorbed isobutene desorbs into the liquid phase as soon as it is produced, and therefore, it has no impact on the total reaction rate. Based on the above, we propose the following kinetic expression,

$$R = k_\mathrm{f}\left[q_\mathrm{TBA}^n - \frac{q_\mathrm{MTBE}\, q_{\mathrm{H_2O}}^n}{K_\mathrm{e}}\right], \quad [8]$$

where R is the reaction rate, q_i is the concentration of component i in the polymer phase, k_f is the forward reaction rate constant, and K_e is the reaction equilibrium constant. The adsorbed phase concentrations, q_i, in Eq. [8] are assumed to follow a linear adsorption relation (Henry's law) in

equilibrium with those in liquid phase:

$$q_i = K_i C_i. \quad [9]$$

The linearity assumption is generally valid at sufficiently low concentration of the reactants and products, as adopted in our experiments. However, at higher concentrations, the multicomponent Langmuir model (29) or the more complicated Flory–Huggins and UNIFAC models (27, 30) must be used in predicting the phase equilibrium on ion-exchange resin.

MATHEMATICAL MODEL

As discussed earlier, the direct etherification reaction between methanol and TBA was visualized as a quasi-homogeneous reaction in the polymer phase considering the large excess of methanol used in the reaction mixture. A new kinetic expression, which combines the three main reactions into one (Eq. [7]), is put forward for convenience in our subsequent studies being conducted at present with a simulated countercurrent moving-bed chromatographic reactor.

A mathematical model based on quasi-homogeneous kinetics was developed, which assumes the reaction in the polymer phase to be homogeneous. The behavior of reactants and products in the fixed-bed reactor was described by a kinetic model, which assumes that the mobile and the stationary phases are always in equilibrium, and the contributions of all the nonequilibrium effects are lumped into an apparent axial dispersion coefficient, D (28). Mass balance equations for each component i (reactants and products) can be written as follows:

$$\frac{\partial C_i}{\partial t} + \left(\frac{l-\varepsilon}{\varepsilon}\right)\frac{\partial q_i}{\partial t} + \frac{u}{\varepsilon}\frac{\partial C_i}{\partial_z} - \left(\frac{1-\varepsilon}{\varepsilon}\right)\nu_i R = D_i \frac{\partial^2 C_i}{\partial z^2}. \quad [10]$$

The initial and boundary conditions are given by

$$C_i[t=0] = C_i^0 \quad [11]$$

$$C_i[0 < t \le t_p]_{z=0} = C_{f,i} \quad [12]$$

$$C_i[t > t_p]_{z=0} = 0 \quad [13]$$

$$\left[\frac{\partial C_i(t)}{\partial z}\right]_{z=0} = 0, \quad [14]$$

where $i =$ TBA, MTBE, H_2O, and u is the superficial fluid phase velocity, which was assumed to be constant. Equation [10] is the overall mass balance equation of each component i in a single packed column and similar to an equation described elsewhere (24). The terms in Eq. [10] are the unsteady state term (the first two terms denote the unsteady state term in the fluid and solid phases, respectively), the convective term (the third term), the reaction term (the fourth term), and the diffusion term (the last term). The apparent dispersion coefficient, D_i, is related to the HETP for the corresponding compounds by (28)

$$D_i = \frac{H_i u}{2} = \frac{Lu}{2N_{ap,i}}. \quad [15]$$

In linear chromatography, HETP is related to the axial dispersion, the adsorption equilibrium, and the coefficients of resistance to mass transfer as described by Van Deemter *et al.* (31). However, determination of the value of the height equivalent to theoretical plate, H_i, or the apparent plate number, $N_{ap,i}$, is a tedious, lengthy process. Hence, in this work, D values are obtained by fitting the experimental elution profiles for each component to the solution of the above model equations (Eqs. [8]–[14]). We have made an additional assumption that the apparent dispersion coefficient for TBA is the same as that for MTBE due to the experimental limitation as there is no way to prevent TBA from undergoing dehydration reaction (Eq. [4]).

The PDE in Eq. [10] together with the initial and boundary conditions (Eqs. [11]–[14]), kinetic model equation (Eq. [8]), and adsorption equilibrium (Eq. [9]) was solved using the method of lines (32). In this technique the PDE is first discretized in space using the finite difference method (FDM) to convert it into a set of several coupled ODE-IVPs. The numerical method of lines combines a numerical method for the initial value problems (IVPs) of ordinary differential equations (ODEs) and a numerical method for the boundary value problems (BVPs). In this work, the resultant stiff ODEs of the initial value kind were solved using the subroutine, DIVPAG (which is based on Gear's method), in the IMSL library. The simulation results obtained from the model describing the concentration profiles of reactants and products are discussed below.

EXPERIMENTAL DETAILS

HPLC grade methanol, MTBE, and TBA have been used in all the experimental runs. The catalyst used is a macroporous sulfonic ion-exchange acid resin, Amberlyst 15 from Rohm & Haas Co. These are cross-linked three-dimensional structures of polymeric material obtained by sulfonation of a copolymer of polystyrene and divinyl benzene. These resin are heat sensitive and lose activity above 393 K. Macroporous resins are better catalysts compared to microporous resins, particularly in nonaqueous media where the latter resins do not swell appreciably. In the MTBE process, the catalyst is poisoned by basic and cationic compounds, which neutralize the active acid groups of the resin. The main properties of the ion-exchange resin (Amberlyst 15) are listed in Table 1. New fresh resin catalysts before use were kept at 368 K in a vacuum oven overnight to get rid of any moisture.

A HPLC column 25 cm long, with an overall volume of 17.35 cm^3, was used in the experimental study. It was packed with 9.66 g of dry resin. A water bath with a temperature

TABLE 1

Typical Properties of Amberlyst 15 Dry Ion-Exchange Resin

Appearance	Hard, dry, spherical particle
Typical particle size distribution	% retained on US standard screens
16 mesh	2–5
16–20 mesh	20–30
20–30mesh	45–55
30–40 mesh	15–25
40–50 mesh	5–10
>50 mesh	1.0
Bulk density, lb/ft^3	38 (608 g/l)
Moisture, by weight	<1%
Hydrogen ion concentration, mequiv/g dry	4.7
Surface area, m^2/g	50
Porosity, ml pore/ml bead	0.36
Average pore diameter, Å	240

controller was used to maintain a constant temperature. A binary, Series 200 LC pump from Perkin-Elmer was connected to the packed bed to provide a rectangular pulse input of width t_p. Effluent from the exit of the column was collected manually at fixed time (2 min) intervals.

Analysis for methanol, TBA, and MTBE was carried out in a HP6890 gas chromatograph equipped with a 30-m-long OV-1 fused silica capillary column from Ohio Valley. A volumetric Karl Fischer titrator with Model 100 titration controller from Denver Instrument was used to measure the concentration of water.

Experiments were conducted at three different temperatures (318, 323, and 328 K) and flow rates. The upper limit of temperature (328 K) was used to maintain MTBE in the liquid phase. Before feeding, the packed bed was first washed with solvent, pure methanol, for about 30 min to drive out the impurities and moisture adsorbed on the resin particle. Then LC pump connected to the feed reservoir was then switched on to continuously provide a rectangular input pulse of width 5–10 min. Afterward, the chemicals adsorbed on the resin catalyst were washed off the column by solvent. It is to be noted that for the reaction studied in this work, methanol, used in the concentration range of 20–24 mol/l, acts as both solvent and reactant. Two sets of experiments were performed. In the first set of experiments, binary mixtures of MTBE and H_2O in methanol were used as feed to study their adsorption and desorption equilibrium in the column. The second set of experiments was conducted to investigate the reaction kinetics. The elution (breakthrough) profiles of the various compounds from the exit of the column were monitored continuously.

RESULTS AND DISCUSSIONS

The first set of experiments conducted was to measure breakthrough curves of MTBE and H_2O when a rectangular pulse of a binary mixture of these two components in methanol (solvent) was injected into the column packed with the Amberlyst 15 resin. No reaction occurs between H_2O and methanol, but MTBE may decompose to isobutene (IB) and methanol on the resin catalyst according to Eq. [6]. However, from the reaction rate expression proposed by Ali and Bhatia (10), the rate of MTBE decomposition is negligible at a low concentration of MTBE and when temperature of the system is low. This assumption was further verified in this work by injecting a rectangular pulse input of MTBE in methanol to the column for 10 min. When a mass balance was performed between the total effluent (area in the breakthrough profile of MTBE) and feed, it was observed that practically no decomposition of MTBE occurred as the discrepancy was only 1.38%. Moreover, no gas bubble (IB) was detected in the effluent. Therefore, adsorption constants, K_{MTBE} and K_{H_2O}, can be determined by fitting model equations described by Eqs. [9]–[14] to the breakthrough curves of MTBE and H_2O.

In order to obtain best-fit (tuned) values of the parameters in the model, an error function, F, is defined. This comprised of a sum of square errors between the experimental and model predicted values,

$$F(p) = \sum_{i=1}^{n} \sum_{j=1}^{m} [C_{ij,\mathrm{exp}} - C_{ij,\mathrm{m}}]^2, \qquad [16]$$

where C_{ij} is the concentration of the ith component for jth data point, p is a vector of parameters tuned, and the subscripts, exp and m, represent experimental values and values predicted by the model, respectively. The state-of-the-art optimization method, the genetic algorithm (GA) (33–35), was used to obtain the values of the model parameters, which minimize the error function, F. GA is a search technique developed by Holland (33) that mimics the process of natural selection and natural genetics. GA is noted for its robustness and the algorithm is superior to traditional optimization algorithms in many aspects (34), and has become quite popular in recent years (35). A short note on GA is added in Appendix A.

DETERMINATION OF ADSORPTION CONSTANTS K_{MTBE} AND K_{H2O}

In the experiments to determine K_{MTBE} and K_{H_2O}, a rectangular pulse input (of width 5 min) of binary mixtures of MTBE and H_2O at low concentration was adopted. Separation of different components takes place due to the difference in their affinity toward the adsorbent, and each component elutes (breakthrough) from the column at a different time. Figure 1 shows experimental as well as model predicted breakthrough curves of MTBE and H_2O at different temperatures. Experimental results show that H_2O travels more slowly than MTBE (less strongly adsorbed) and there is some band broadening. The reasons for the broadening

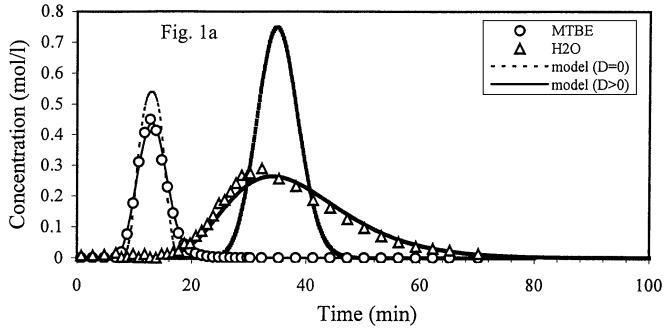

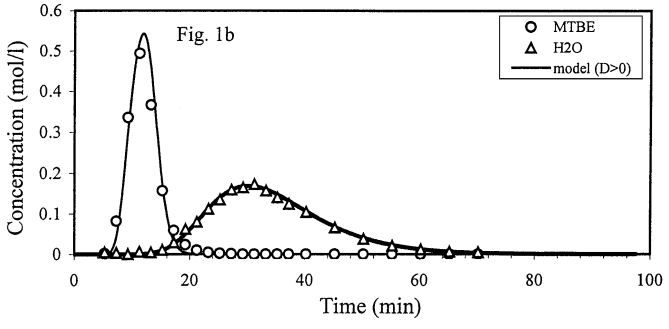

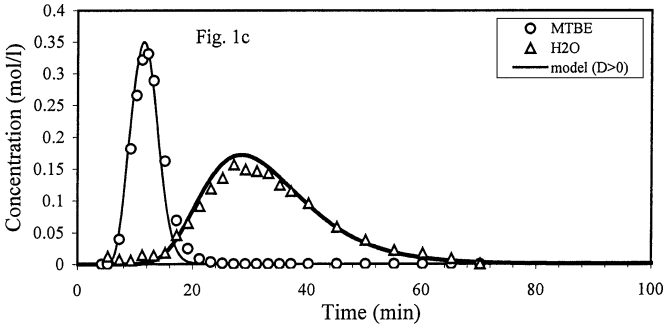

FIG. 1. Effect of temperature on breakthrough curve of the MTBE–H_2O system. Symbols, experiment; lines, model prediction (for all the figures, if not specified). Experimental conditions: flow rate $Q = 1$ ml/min, $t_p = 5$ min. (a) $T = 318$ K, $C_{f,\,MTBE} = 0.5488$ mol/l, $C_{f,\,H_2O} = 1.34$ mol/l; (b) $T = 323$ K, $C_{f,\,MTBE} = 0.6114$ mol/l, $C_{f,\,H_2O} = 0.79$ mol/l; (c) $T = 328$ K, $C_{f,\,MTBE} = 0.4104$ mol/l, $C_{f,\,H_2O} = 0.799$ mol/l.

are manifold: mass transfer resistance, adsorption, and axial dispersion are among the most important factors. In this work, for simplicity, these factors were lumped into one parameter, namely, the apparent axial dispersion coefficient, D (see Eq. [10]). For the nonreactive case (MTBE–H_2O system), Eq. [10] simplifies to

$$\frac{\partial C_i}{\partial t} + \left(\frac{1-\varepsilon}{\varepsilon}\right)\frac{\partial q_i}{\partial t} + \frac{u}{\varepsilon}\frac{\partial C_i}{\partial z} = D_i\frac{\partial^2 C_i}{\partial z^2}, \qquad [17]$$

where i = MTBE, H_2O. The objective function F (Eq. [16]) was minimized by tuning four parameters, p, namely, K_{MTBE}, K_{H_2O}, D_{MTBE}, and D_{H_2O}, to match the model prediction to the experimental breakthrough curves. The tuned adsorption and dispersion parameters for MTBE and H_2O obtained by fitting the model to experimental results are

TABLE 2

Adsorption Equilibrium Constants and Apparent Dispersion Coefficients for MTBE and H_2O

T, K	K_{MTBE}	K_{H_2O}	$10^6 D_{MTBE}$	$10^6 D_{H_2O}$	F
318	0.375	2.846	1.948	7.092	0.014
323	0.330	2.800	2.333	7.708	0.030
328	0.300	2.750	2.350	8.167	0.014

tabulated in Table 2 and are compared to experimental results in Fig. 1 for three different temperatures. Figure 1a shows that model prediction is quite good when $D \neq 0$ compared to when D is set equal to zero. The minimum values of the error function F in Eq. [16] obtained are 0.547 and 0.014 for $D = 0$ and $D \neq 0$ respectively. It is obvious that model prediction is worse when the dispersion term is neglected.The presence of a dispersion term in Eq. [17] is, therefore, indispensable in predicting breakthrough curves accurately. The adsorption equilibrium constant of water was found out to be about 10 times greater than the corresponding value for MTBE (Table 2). This is expected due to the stronger polarity of H_2O. Table 2 also shows that the adsorption equilibrium constants for both MTBE and H_2O decrease with temperature while the dispersion coefficients increase.

At low concentrations, the model results fit the experimental breakthrough curve very well. However, the linear adsorption isotherm is less accurate in predicting the elution profile when the solute is present at high concentration. When a mixture of $[MTBE]_f = 0.54$ mol/l and $[H_2O]_f = 1.328$ mol/l was injected with a pulse width of 20 min, which is comparatively larger than the experimental conditions for Fig. 1a, it was observed that a model using the K and D values of Table 2 cannot predict accurately the experimentally observed breakthrough curves, particularly for H_2O. This is shown in Fig. 2. Although model prediction for MTBE is quite good, it shows

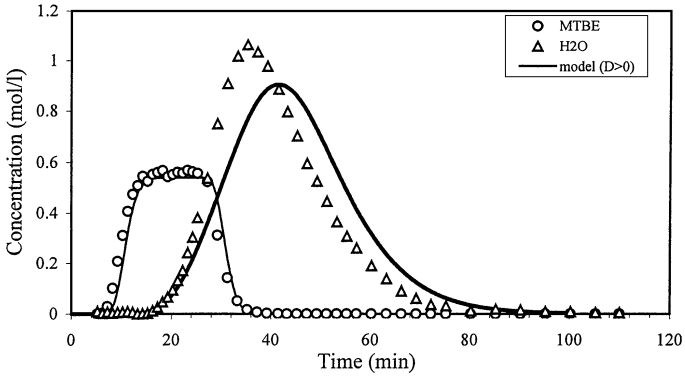

FIG. 2. Effect of nonlinearity on the breakthrough curve of the MTBE–H_2O system. Experimental conditions: $Q = 1$ ml/min; $t_p = 20$ min; $T = 318$ K, $C_{f,\,MTBE} = 0.54$ mol/l, $C_{f,\,H_2O} = 1.328$ mol/l.

that due to the tailing effect prediction for H_2O is poor, and a nonlinear adsorption isotherm must be considered. Figure 2 also reveals that at higher concentrations, the migration velocity obtained experimentally is larger than that of the model predicted value (using linear isotherm constants) as can be seen from the difference in the retention time of the concentration peak between model and experimental profiles. These effects indicate that adsorption of H_2O on the Amberlyst 15 resin follows a convex upward isotherm, where dq/dC decreases with increasing concentration.

DETERMINATION OF ADSORPTION CONSTANT, K_{TBA}, AND REACTION PARAMETERS, k_f, K_e, AND n

Experiments were conducted at three different temperatures by feeding a rectangular pulse (10 min width) input of TBA of a certain concentration in methanol. Pure methanol (solvent) was continuously pumped into the column to wash away any unconverted TBA and products MTBE and H_2O out of the packed-bed reactor. Adsorption constant K_{TBA} and reaction kinetic parameters k_f, K_e, and n were determined from these reactive experiments, by minimizing Eq. [16]. The model equations used for tuning four parameters (K_{TBA}, k_f, K_e, and n) are Eqs. [10]–[14] together with the kinetic expression (Eq. [8]) and the linear adsorption isotherm (Eq. [9]). In solving the model equations, the values of K_{MTBE}, K_{H_2O}, D_{MTBE} and D_{H_2O} obtained earlier (given in Table 2) were used unchanged. In addition, D_{TBA} was assumed to be equal to D_{MTBE}. The four parameters K_{TBA}, k_f, K_e and n) were tuned at each of the three temperatures using the genetic algorithm that minimizes the error function defined in Eq. [16]. The tuned values of the four parameters at different temperatures are listed in Table 3. The equilibrium conversion of TBA and the yield, selectivity, and purity of MTBE for three different temperatures are also reported in Table 3. The experimental and model predicted results (using the values of Tables 2 and 3) are shown in Fig. 3. Once again, the proposed model can predict the experimental breakthrough curves reasonably well when $D \neq 0$.

The single objective function optimization problem involving minimization of the error function was solved using the genetic algorithm. A gene pool of 50 chromosomes was considered and GA operations were carried out for 50 generations, after which it was observed that all 50 chromosomes converged to a single global optimum. The CPU time

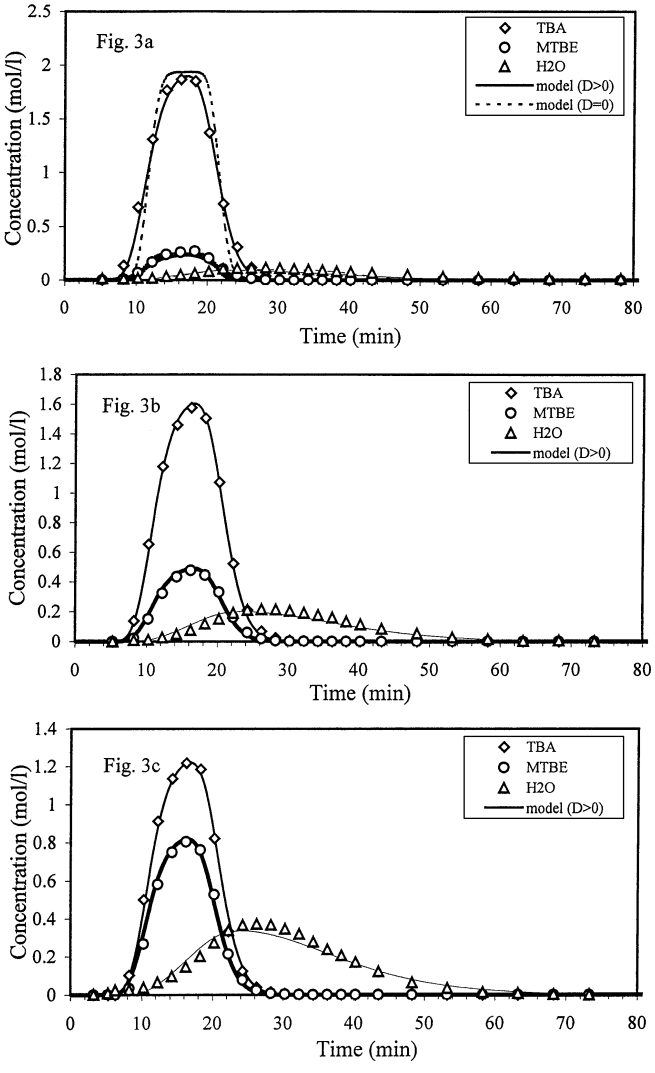

FIG. 3. Effect of temperature on the breakthrough curves of the TBA–H_2O–MTBE system. Experimental conditions: $Q = 1$ ml/min, $t_p = 10$ min, $C_{f,TBA} = 2.189$ mol/l. (a) $T = 318$ K; (b) $T = 323$ K; (c) $T = 328$ K.

TABLE 3

Adsorption Equilibrium Constant, K_{TBA}, and Kinetic Parameters, k_f, K_e, and n

T, K	K_{TBA} (–)	k_f, $mol^{(1-n)} \cdot l^{(n-1)}$/min	K_e, mol/l	n, (–)	F, mol/l	X_{TBA},[a] (–)	Y_{MTBE},[a] (–)	S_{MTBE},[a] (–)	P_{MTBE},[a] (–)
318	0.460	0.025	24.682	1.018	0.056	0.8839	0.8683	0.4955	0.4648
323	0.440	0.060	20.943	1.092	0.026	0.8586	0.7863	0.4780	0.4402
328	0.460	0.112	18.202	1.120	0.048	0.8524	0.7611	0.4717	0.4322

[a] Calculation is based on $[TBA]_o = 1.5$ mol/l. $X_{TBA} = 1 - [TBA]_{out}/[TBA]_o$; $Y_{MTBE} = [MTBE]_{out}/[TBA]_o$; $S_{MTBE} = [MTBE]_{out}/([MTBE]_{out} + [H_2O]_{out})$; $P_{MTBE} = [MTBE]_{out}/([MTBE]_{out} + [H_2O]_{out} + [TBA]_{out})$.

required for 50 generations was 600 min on the CRAY J916 supercomputer.

In the heterogeneous reaction sequence, mass transfer of reactants first takes place from the bulk fluid to the external surface of the pellet. The reactants then diffuse from the external surface into and through the pores within the pellet. In order to determine intrinsic kinetic parameters, the effect of bulk diffusion resistance and pore diffusion resistance must be estimated first.

Estimation of Bulk (External) Diffusion Resistance

Mears's criterion (36, 41), which uses the measured rate of reaction, helps to determine if external diffusion is limiting the reaction. Mears's criterion states that external mass transfer can be neglected if

$$\frac{(-r'_{\mathrm{A}}\rho_{\mathrm{b}})Rn}{k_{\mathrm{c}}C_{\mathrm{A}}} < 0.15, \qquad [18]$$

where $(-r'_{\mathrm{A}}\rho_{\mathrm{b}})$ is the measured rate of reaction, in kilomoles per cubic meter peer second, R is the average radius of catalyst particles (3.75×10^{-4} m), n is the order of reaction, C_{A} is the bulk concentration of the reactant (TBA), in kilomoles per cubic meter, and k_{c} is the mass transfer coefficient, in meters per second. The measured rate of reaction can be determined from Eq. [8] as 0.381 kmol/m^3-catalyst bed/s, and the mass transfer coefficient, k_{c}, can be estimated from the Dwidevi–Upadhyay mass transfer correlation (42) as 3.49×10^{-5} m/s, which results in Mears's criterion parameter value as 2.98×10^{-3}, which is less than 0.15. Therefore, bulk diffusion can be neglected. It should also be noted that estimated kinetic parameters as reported in Table 3 can predict the breakthrough curves very well when experiments were performed at other flow rates, confirming further that external mass transfer resistance is negligible. Detailed calculation is shown in Appendix B.

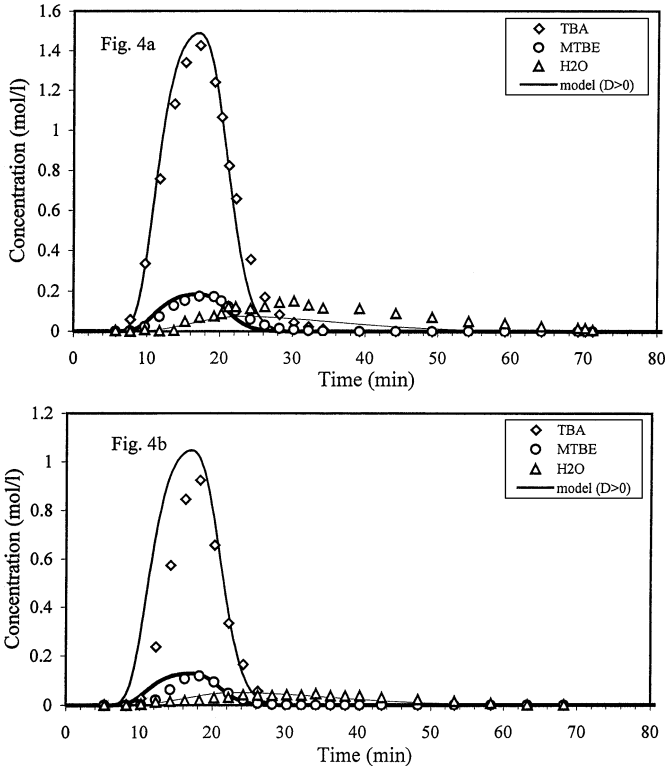

FIG. 4. Effect of feed concentration on the breakthrough curves of the TBA–H_2O–MTBE system. Experimental conditions: $T = 318$ K, $Q = 1$ ml/min, $t_{\mathrm{p}} = 10$ min, (a) $C_{\mathrm{f,TBA}} = 1.7117$ mol/l; (b) $C_{\mathrm{f,TBA}} = 1.203$ mol/l.

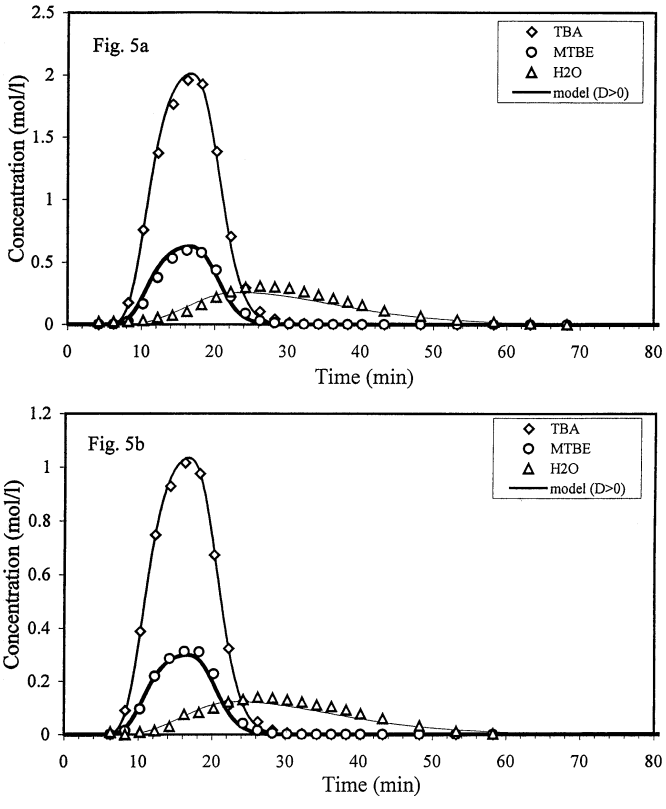

FIG. 5. Effect of feed concentration on the breakthrough curves of the TBA–H_2O–MTBE system. Experimental conditions: $T = 323$ K, $Q = 1$ ml/min, $t_{\mathrm{p}} = 10$ min. (a) $C_{\mathrm{f,TBA}} = 2.766$ mol/l; (b) $C_{\mathrm{f,TBA}} = 1.398$ mol/l.

Estimation of Pore Diffusion Resistance

The Weisz–Prater criterion is used to determine whether internal mass transfer is limiting the reaction.The Weisz–Prater criterion (36) states that internal pore diffusion is negligible if

$$\frac{[-r'_{\mathrm{A}}\rho_{\mathrm{b}}]_{\mathrm{obs}}L^2}{D_{\mathrm{e}}C_{\mathrm{As}}} < 1, \qquad [19]$$

where C_{As} is the concentration of TBA on the resin surface, D_{e} is the effective diffusivity of TBA in methanol, and L for a spherical pellet is given by $R/3$, where R is the average radius of the resin particles. The Weisz–Prater parameter

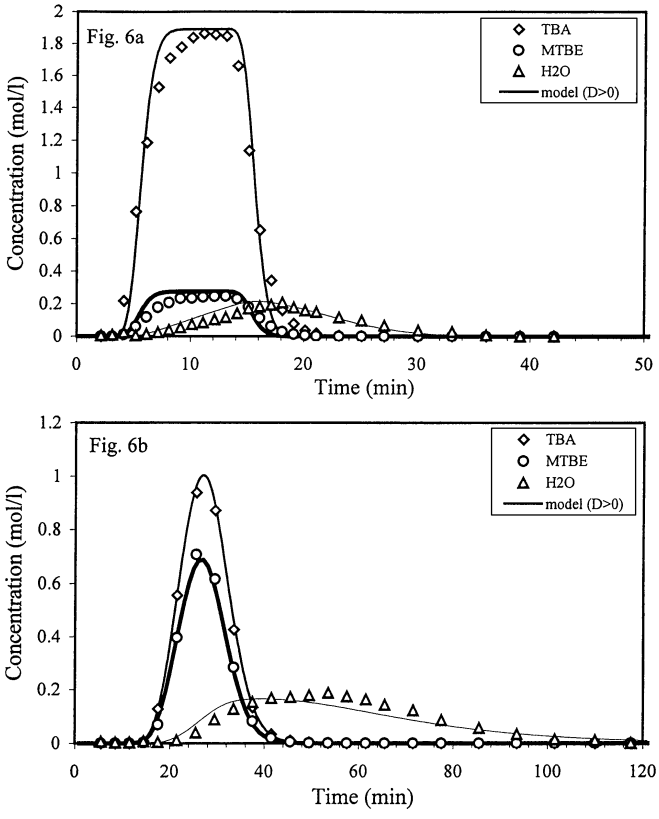

FIG. 6. Effect of flow rate on the breakthrough curves of the TBA–H_2O–MTBE system. Experimental conditions: $T = 323$ K, $C_{f,\,TBA} = 2.189$ mol/l, $t_p = 10$ min. (a) $Q = 2$ ml/min; (b) $Q = 0.5$ ml/min.

calculated (see Appendix B) for the given system yields a value of 0.012, signifying that internal pore diffusion is also negligible.

The tuned adsorption and kinetic parameters of the three components at three different temperatures were used next to verify the validity of the model by checking whether it can correctly predict experimental breakthrough curves of the three components when experiments were performed at different flow rates and feed concentrations. Figure 4 shows results obtained when feed concentrations were varied keeping the temperature at 318 K and flow rate at 1 ml/min, the same values as in Fig. 3a. Figure 5 shows a similar effect of feed concentrations at $T = 323$ K while Fig. 6 compares model predicted values to experimental results at different flow rates. These figures show that when adsorption and kinetic parameter values of Tables 2 and 3 are used the model can predict quite well the breakthrough curves of all three components, particularly for MTBE and TBA. From the figures it is also apparent that when reaction occurs broadening of the elution peaks is less significant as the overall rate is controlled by kinetics (rate-determining step) rather than by axial dispersion. The main reason for the small error is believed to be that we have neglected the varied degree to which the resin gets swollen when concentration changes inside the packed-bed reactor. As a result, the local voidage will change, which subsequently changes the interfacial flow velocity. However, considering the low concentration range adopted in this work, the concentration change is relatively small, and the error caused is insignificant.

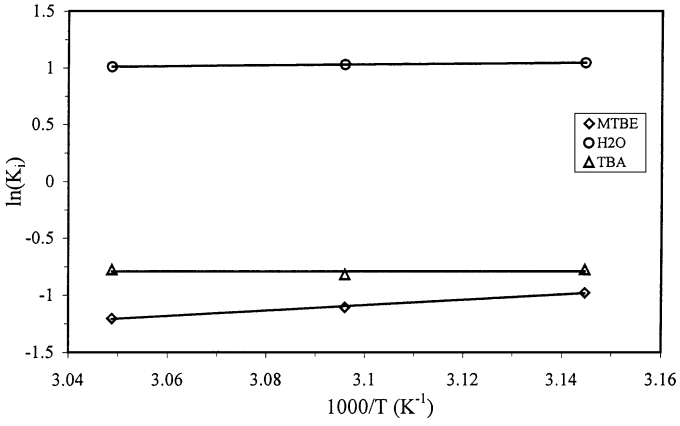

FIG. 7. Temperature dependence of adsorption constants.

The dependence of adsorption constants, K_{MTBE}, K_{H_2O}, and K_{TBA}, on temperature can be determined from the equation,

$$K_i = K_{i,o} \exp\left[\frac{-\Delta H_i}{RT}\right], \qquad i = \text{MTBE, } H_2O\text{, TBA,} \quad [20]$$

where ΔH is the heat of adsorption. The heat of adsorption is exothermic ($\Delta H_i < 0$), and therefore, K_i decreases with increase of temperature. The values of $K_{i,o}$ and ΔH_i were obtained for each component (MTBE, H_2O, and TBA) by least-squares fitting as shown in Fig. 7. It was observed that the effect of temperature is not significant in the temperature range under study. The values of $K_{i,o}$ and ΔH_i for TBA, MTBE, and H_2O are given in Table 4. In order to verify the thermodynamic consistency, enthalpy, and entropy of adsorption of the components, the standard states were changed to 1 atm in the gas phase. The calculations made were identical to those reported by Boudart (37) and Singh and Vannice (38). The standard states for ΔH and ΔS were changed from liquid at 1 mol to pure gas at 1 atm by following the path shown by Singh and Vannice (38). The enthalpy and entropy of adsorption of MTBE and methanol were found to be negative as required by thermodynamics

TABLE 4

Pre-exponential Factors and Heat of Adsorption

$K_{i,o}$			ΔH_i, J/mol		
TBA	MTBE	H_2O	TBA	MTBE	H_2O
0.446	2.461×10^{-4}	0.924	39.9	19363.3	2974.7

TABLE 5

Comparison of Thermodynamic Parameters for Liquid and Vapor Phase Studies at Standard State of 1 atm

	Liquid phase		Vapor phase	
	$-\Delta H^o$, kJ/mol	ΔS^o, kJ/mol/K	$-\Delta H^o$, kJ/mol	ΔS^o, kJ/mol/K
K_{MTBE}	18.6	−59	20.3	−48
K_{TBA}	0.03	−16	0.04	−8
K_{H_2O}	3	−38	1.7	−29

and are given in Table 5. It is interesting to note the common trends between the liquid and vapor phase values reported in Table 5 and the fitted values obtained as reported in Table 4. Some of the values do differ slightly between the liquid and vapor phases but they all satisfy thermodynamic constraints. It should also be noted that this is the only study where synthesis of MTBE is done from TBA and methanol. All other MTBE synthesis studies reported in the literature are from isobutene (IB) and methanol and Refs. (39, 40) did not report enthalpy and entropy of adsorption in their reported work. In addition, in these works Lewatit SPC 118 BG was used as adsorbent and catalyst instead of the Amberlyst 15 used in this work.

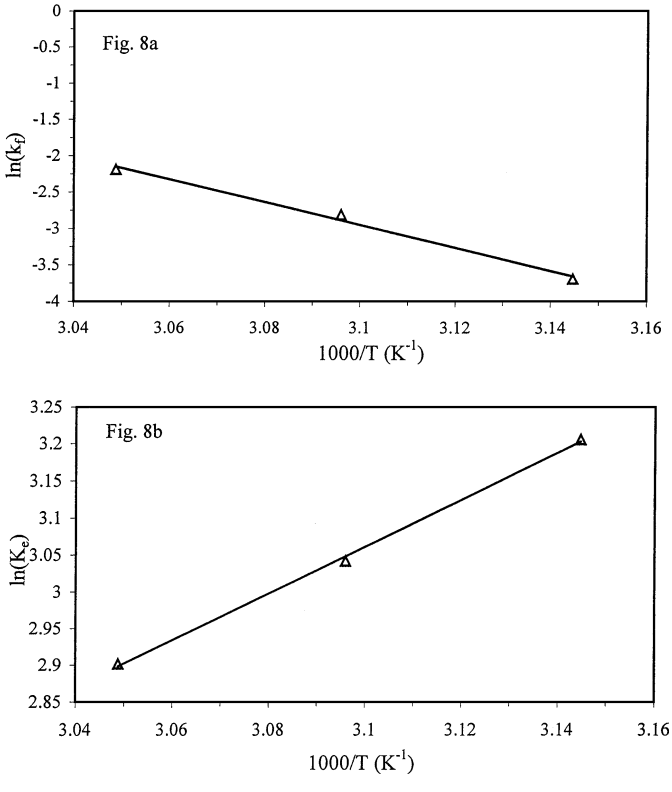

FIG. 8. Effects of temperature on (a) k_f and (b) K_e.

TABLE 6

Reaction Kinetic Parameters

$k_{f,o}$, $mol^{(1-n)} \cdot l^{(n-1)}$/min	E_f, kJ/mol	ΔS^o_R, J/mol/K	$-\Delta H^o_R$, kJ/mol
6.028×10^{19}	130.147	−56.444	26.418

The dependence of the forward reaction rate constant K_f on temperature was determined from the Arrhenius equation,

$$k_f = k_{f,o} \exp\left[\frac{-E_f}{RT}\right]. \quad [21]$$

The values of activation energy, E_f, and pre-exponential factor, $k_{f,o}$ were obtained from the slope of the trend line (shown in Fig. 8) and the values are given in Table 6. The reaction equilibrium constant, K_e, is related by

$$k_e = \left[\frac{k_f}{k_b}\right] = \left[\frac{k_{f,o}}{k_{b,o}}\right] \exp\left[-\frac{(E_f - E_b)}{RT}\right] = \exp\left[-\frac{\Delta G^o_R}{RT}\right]$$
$$= \exp\left[\frac{\Delta S^o_R}{R}\right] \exp\left[-\frac{\Delta H^o_R}{RT}\right]. \quad [22]$$

The values of $\Delta S^o_R[\equiv R \ln(\frac{k_{f,o}}{k_{b,o}})]$ and $\Delta H^o_R[\equiv(E_f - E_b)]$ were obtained by least-squares fitting and the values are given in Table 6. The effect of temperature on kinetic parameter n, which represents the ratio of the production rate of H_2O to that of MTBE, is shown in Table 3. n increases with increasing temperature, indicating that more H_2O and IB is produced than MTBE at higher reaction temperature. The ΔH^o_R and ΔS^o_R values obtained in this work (see Table 6) differ from the value reported by Izqulerdo *et al.* (39, 40). They reported $-\Delta H^o = 37.1$ kJ/mol and $\Delta S^o = -79.3$ J/mol/K compared to our values of 26.42 kJ/mol and −56.44 J/mol/K, respectively. However, it should be noted that they considered MTBE synthesis reaction from isobutene (IB) and methanol, whereas in this work we considered synthesis of MTBE by a different route, namely, direct reaction of TBA with methanol. Moreover, they reported large discrepancies of values of $-\Delta H^o_R$ at different temperatures.

CONCLUSIONS

Synthesis of MTBE by direct reaction between methanol and TBA on acid ion-exchange resin, Amberlyst 15, packed in a reactor is studied in the temperature range of 318–328 K and at different flow rates. Methanol also acts as solvent and is used in excess. The reaction was visualized as a quasi-homogeneous reaction in the polymer phase, and is assumed to be in (adsorption) equilibrium with that of the liquid phase. The adsorption equilibrium was described by a linear isotherm as only the low concentration range was

considered. A new kinetic expression was established. The breakthrough curves of the reactants and products were experimentally measured at different temperatures, feed concentrations, and flow rates. Experimental results show that H_2O travels more slowly than MTBE (less strongly adsorbed), the reaction rate increases with an increase in reaction temperature, and the conversion of the limiting reactant, TBA, is favored at high temperatures and at low flow rates of TBA. The adsorption equilibrium constants and reaction kinetic parameters together with their dependence on temperature were determined by least-squares fitting of the proposed model to the experimental results using a state-of-the-art optimization technique, the genetic algorithm. Pure kinetic parameters were obtained as it was found that under the experimental conditions used, both external and internal mass resistances are negligible. The adsorption constant of H_2O was found to be almost 10 times greater than that of MTBE and as a result, the desired product MTBE always elutes faster than H_2O. The effects of temperature on forward reaction constant, k_f, and reaction equilibrium constant, K_e, were also explored. The activation energy for this reaction was determined to be 130.1 kJ/mol. The fitted parameters obtained for enthalpy and entropy of adsorption from Arrhenius plots were found to be consistent with thermodynamics when the standard states were changed to liquid at 1 mol to pure gas at 1 atm. The accuracy of the proposed mathematical model was further verified when it was observed that the model could predict experimental results at different feed concentrations and flow rates quite well.

APPENDIX A: A NOTE ON GENETIC ALGORITHM

GA is a search technique developed by Holland (33) that mimics the process of natural selection and natural genetics. In this algorithm, a set of decision variables are first coded in the form of a set of randomly generated binary numbers (0 and 1), called *strings* or *chromosomes*, thereby creating a "population (gene pool)" of such binary strings. Each chromosome is then mapped into a set of *real* values of the decision variables, using the upper and lower bounds of each of these. A model of the process is then used to provide values of the objective function for each chromosome. The value of the objective function of any chromosome reflects its "fitness." The Darwinian principle of "survival of the fittest" is used to generate a new and improved gene pool (new generation). This is done by preparing a "mating pool," comprising copies of chromosomes, the number of copies of any chromosome being proportional to its fitness (Darwin's principle). Pairs of chromosomes are then selected randomly, and pairs of daughter chromosomes generated using operations similar to those in genetic reproduction. The gene pool evolves, with the fitness improving over the generations.

Three common operators are used in GA to obtain an improved (next) generation of chromosomes. These are referred to as reproduction, crossover, and mutation. Reproduction is the generation of the mating pool, where the chromosomes are copied probabilistically on the basis of their fitness values. However, no new strings are formed in the reproduction phase. *New* strings are created using the crossover operator by exchanging information among pairs of strings in the mating pool. A pair of daughter chromosomes are produced by selecting a crossover site (chosen randomly) and exchanging the two parts of the pair of parent chromosomes (selected randomly from the mating pool). The effect of crossover may be detrimental or beneficial. It is hoped that the daughter strings are superior. If they are worse than the parent chromosomes, they will slowly die a natural death over the next few generations (the Darwinian principle at work). In order to preserve some of the good strings that are already present in the mating pool, not all strings in the pool are used in crossover. A crossover probability, P_{cross}, is used, where only $100P_{cross}$ percent of the strings in the mating pool are involved in crossover while the rest continue unchanged to the next generation. After a crossover is performed, mutation takes place. The mutation operator changes a binary number at *any* location in a chromosome from a 1 to a 0 and vice versa, with a small probability, P_{mute}. Mutation is needed to create a point in the neighborhood of the current point, thereby achieving a local search around the current solution and maintaining diversity in the population. The entire process is repeated until some termination criterion is met (the specified maximum number of generations is attained, or the improvements in the values of the objective functions become lower than a specified tolerance). A more elaborate description of GA is available in the works Holland (33), Goldberg (34), and Bhaskar *et al.* (35).

APPENDIX B. ESTIMATION OF EXTERNAL AND INTERNAL MASS TRANSFER RESISTANCE

Estimation of External Mass Transfer

Mears's criterion (41) is given by

$$\frac{(-r'_A\rho_b)Rn}{k_c C_A} < 0.15, \qquad [B1]$$

where $(-r'_A\rho_b)$ is the measured rate of the reaction based on the bulk volume of packed bed, in kilomoles per cubic meter of catalyst bed per second. The initial reaction rate is given by

$$\begin{aligned}(-r'''_A)_{obs} = k_f q_{TB}^n &= (0.06)[(0.44)(1.5)]^{1.092}[10^3/60]\\ &= 0.635\ \text{mol/m}^3\ \text{catalyst/s}\\ &= 0.381\ \text{mol/(m}^3\ \text{catalyst bed)/s}.\end{aligned}$$

The mass transfer coefficient was calculated from the Dwidevi and Upadhyay correlation (42) which is valid for liquids ($Re > 0.01$) in fixed beds and is given by

$$\varepsilon_b J_D = \frac{\varepsilon_b Sh}{Sc^{1/3} Re} = \frac{0.765}{Re^{0.82}} + \frac{0.365}{Re^{0.386}}, \qquad [B2]$$

where

$$Re = \frac{U\rho_{MeOH} d_p}{\mu_{MeOH}} = \frac{(0.00024\,\text{m/s})(790\,\text{kg/m}^3)(0.00075\,\text{m})}{(0.0006\,\text{kg/m}\cdot\text{s})} = 0.237 > 0.01,$$

where U = superficial velocity of fluid through bed = 0.00024 m/s, and d_p = average catalyst particle diameter = 0.00075 m.

Schmidt number

$$Sc = \frac{\mu}{\rho D_{AB}} = \frac{(0.0006\,\text{kg/m}\cdot\text{s})}{(790\,\text{kg/m}^3)(1.93\times10^{-9}\,\text{m}^2/\text{s})} = 393.52.$$

Substituting into Eq. [B2], we have $Sh = k_c d_p / D_{AB} = 13.578$. D_{AB} can be obtained from the Wilke–Chang equation (36) as

$$D_{AB} = \frac{(117.3\times10^{-18})(\varphi M_B)^{0.5} T}{\mu v_A^{0.6}}\,\text{m}^2/\text{s},$$

where $\varphi = 1.9$ (methanol), $M_B = 32$ kg/kmol, $T = 323$ K, $\mu = 0.0006$ kg/ms (methanol), v_A = molar volume at normal boiling point of TBA $= 0.285(V_c)^{1.048} = 0.10263$ m^3/kmol. Substituting, we have $D_{AB} = 1.93\times10^{-9}$ m^2/s. Therefore, the mass transfer coefficient, $k_c = 3.49\times10^{-5}$ m/s. Substituting in Mears's criterion parameter, we have

$$\frac{(r'_A\rho_b)Rn}{k_c C_A} = \frac{(0.381)(0.000375)(1.092)}{(3.49\times10^{-5})(1500)} = 2.98\times10^{-3} < 0.15.$$

Therefore, external mass transfer (bulk diffusion) can be neglected.

Estimation of Internal Mass Transfer

The Wiesz–Prater criterion is used to determine whether internal mass transfer is limiting the reaction.The Wiesz–Prater criterion (36) states that internal pore diffusion is negligible if

$$\frac{[r'_A\rho_b]_{obs} L^2}{D_e C_{As}} < 1, \qquad [B3]$$

where C_{As} is the concentration of TBA on the resin surface. Since bulk diffusion is negligible, C_{As} can be taken as $C_A = 1500$ mol/m^3. D_e is the effective diffusivity of TBA in methanol, and is given by $[\varepsilon/\tau]\,D_{AB}$, where ε is particle porosity = 0.36 (Table 1), t is tortuosity factor = 1.3 (43). $L = R/3$, for a spherical pellet where R is the average radius of the resin particles. Substituting in Eq. [B3], we have Weisz–Prater parameter = 0.012, signifying that internal pore diffusion is negligible.

NOTATION

C	liquid phase concentration, mol/l
D	apparent axial dispersion coefficient, m^2/s
E	activation energy, J/mol
F	error (objective) function for optimization
ΔG	change in Gibbs free energy of reaction, J/mol
H	height equivalent to a theoretical plate, m
ΔH	heat of adsorption, J/mol
IB	isobutene
k	reaction rate constant
K	equilibrium constant
L	length of the packed bed reactor, m
MeOH	methanol
MTBE	methyl *tert*-butyl ether
n	moles of TBA reacted per mole of methanol
N	equivalent plate number
P	vector of parameters tuned
q	concentration in the polymer phase, mol/l
R	reaction rate, mol/min/l, universal gas constant
ΔS	entropy change of reaction, J/mol/K
t	time, s
T	temperature, K
TBA	*tert*-butyl alcohol
u	superficial fluid phase flow rate, m/s
z	axial coordinate, m

Greek Letters

ε	void fraction
ν	stoichiometric coefficient of component

Subscripts/Superscripts

o	initial, pre-exponential, standard
ap	apparent
b	backward
e	equilibrium
exp	experiment
f	feed, forward
i	component i
j	data point
m	model, number of data points
n	exponent, number of components
p	width of rectangular pulse

REFERENCES

1. Peeples, J. E., *Fuel Reform.* **1**(1), 27 (1991).
2. Hadder, G. R., *Energy* **21**, 118 (1992).
3. Swain, E. J., *Oil Gas J.* **97**(24), 99 (1999).

4. Ancillotti, F., Massi Mauri, M., and Pescarollo, E., *J. Catal.* **46**, 49 (1977).
5. Ancillotti, F., Massi Mauri, M., Pescarollo, E., and Romagnoni, L., *J. Mol. Catal.* **4**, 37 (1978).
6. Gicquel, A., and Torck, B., *J. Catal.* **83**, 9 (1983).
7. Voloch, M., Ladisch, M. R., and Tsao, G. T., *React. Polym.* **4**, 91 (1986).
8. Subramanium, C., and Bhatia, S., *Can. J. Chem. Eng.* **65**, 613 (1987).
9. Al-Jarallah, A. M., Siddiqui, M. A. B., and Lee, A. K. K., *Can. J. Chem. Eng.* **66**, 802 (1988).
10. Ali, A., and Bhatia, S., *Chem. Eng. J.* **44**, 97 (1990).
11. Rehfinger, A., and Hoffmann, U., *Chem. Eng. Sci.* **45**, 1605 (1990).
12. Parra, D., Tejero, J., Cunill, F., Iborra, M., and Izquierdo, J. F., *Chem. Eng. Sci.* **49**, 4563 (1994).
13. Izquierdo, J. F., Cunill, F., Vila, M., Iborra, M., and Tejero, J., *Ind. Eng. Chem. Res.* **33**, 2830 (1994).
14. Caetano, N. S., Loureiro, J. M., and Rodrigues, A. E., *Chem. Eng. Sci.* **49**, 4589 (1994).
15. Tejero, J., Cunill, F., Izquierdo, J. F., Iborra, M., Fité, C., and Parra, D., *Appl. Catal. A-Gen.* **134**, 21 (1996).
16. Chu, P., and Kuhl, G. H., *Ind. Eng. Chem. Res.* **26**, 365 (1987).
17. Kogelbauer, A., Nikolopoulos, A. A., Goodwin, Jr., J. G., and Marcelin, G., *J. Catal.* **152**, 122 (1995).
18. Collignon, F., Loenders, R., Martens, J. A., Jacobs, P. A., and Poncelet, G., *J. Catal.* **182**, 302 (1999).
19. Horvath, T., Seiler, M., and Hunger, M., *Appl. Catal. A-Gen.* **193**, 227 (2000).
20. Ali, M. A., Brisdon, B. J., and Thomas, W. J., *Appl. Catal. A-Gen.* **197**, 303 (2000).
21. Sugiyama, K., Kato, K., Miura, H., and Matsuda, T., *J. Jpn. Petrol. Inst.* **26**, 243 (1983).
22. Knifton, J. F., and Edwards, J. C., *Appl. Catal. A-Gen.* **183**, 1 (1999).
23. Matouq, M. H., and Shigeo, G., *Int. J. Chem. Kinet.* **25**, 825 (1993).
24. Ray, A. K., Carr, R. W., and Aris, R., *Chem. Eng. Sci.* **49**(4), 469 (1994).
25. Ray, A. K., and Carr, R. W., *Chem. Eng. Sci.* **50**(14), 2195 (1995).
26. Colombo, F., Corl, L., Dalloro, L., and Delogu, P., *Ind. Eng. Chem. Fundam.* **22**(2), 219 (1983).
27. Mazzotti, M., Kruglov, A., Neri, B., Gelosa, D., and Morbidelli, M., *Chem. Eng. Sci.* **51**, 1827 (1996).
28. Guiochon, G., Shirazi, S. G., and Katti, A. M., "Fundamentals of preparative and nonlinear chromatography." Academic Press, Boston, 1994.
29. Migliorini, C., Fillinger, M., Mazzotti, M., and Morbidelli, M., *Chem. Eng. Sci.* **54**, 2475 (1999).
30. Mazzotti, M., Neri, B., Gelosa, D., Kruglov, A., and Morbidelli, M., *Ind. Eng. Chem. Res.* **36**, 3 (1997).
31. Van Deemter, J. J., Zuiderweg, F. J., and Klinkenberg, A., *Chem. Eng. Sci.* **5**, 271 (1956).
32. Schiesser, W. E., "The Numerical Method of Lines." Academic Press, New York, 1991.
33. Holland, J. H., "Adaptation in natural and artificial systems." Univ. Michigan Press, Ann Arbor, MI, 1975.
34. Goldberg, D. E., "Genetic algorithms in search, optimization and machine learning." Addison-Wesley, Reading, MA, 1989.
35. Bhaskar, V., Gupta, S. K., and Ray, A. K., *Rev. Chem. Eng.* **16**(1), 1 (2000).
36. Fogler, H. C., "Elements of Chemical Reaction Engineering." Prentice-Hall, Englewood Cliffs, NJ, 1986.
37. Boudart, M., *AIChE J.* **18**(3), 465 (1972).
38. Singh, U. K., and Vannice, M. A., *AIChE J.* **45**(5), 1059 (1999).
39. Izqulerdo, J. F., Cunill, F., Vlla, M., Tejero, J., and Iborra, M., *J. Chem. Eng. Data* **37**, 339 (1992).
40. Izqulerdo, J. F., Cunill, F., Vlla, M., Iborra, M., and Tejero, J., *Ind. Eng. Chem. Res.* **33**, 2830 (1994).
41. Mears, D. F., *Ind. Eng. Chem. Process Des. Dev.* **10**, 541 (1971).
42. Dwidevi, P. N., and Upadhyay, S. N., *Ind. Eng. Chem. Process Des. Dev.* **16**, 157 (1977).
43. Rehfinger, A., and Hoffmann, U., *Chem. Eng. Sci.* **45**, 1619 (1990).